Article ID 1004-924X(2005)05-0575-09

Adaptive segmentation of digital mammograms through reinforcement learning

LIU Xin-yue[1], FANG Xiao-xuan[2], HUANG Lian-qing[1]

(1. *Changchun Institute of Optics, Fine Mechanics and Physics, Chinese Academy of Sciences, Changchun* 130033, *China*; 2. *China-Japan Union Hosptial of Jilin University, Changchun* 130033, *China*)

Abstract: An approach based on reinfocement learning for the automated segmentation is presented. The approach consists of two modules: segmentation module and learning module. The segmentation module uses the region-growing algorithm combined with the smooth filtering and the morphological filtering to segment mammograms. The learning module uses the segmentation output as the feedback to learn to select the optimal parameter settings of the segmentation algorithm according to the image properties using reinforcement learning techniques. The approach can adapt itself to various kinds of mammograms through training and therefore obviates the tedious and error-prone tuning of parameter settings manually. Quantitative test results show that the approach is accurate for several kinds of mammograms. Compared to previously proposed approaches, the approach is more adaptable to different mammograms.

Key words: adaptive image segmentation; digital mammography; reinforcement learning

1 Introduction

Computer-aided diagnosis of mammograms[1-2] uses the output of the computerized analysis of mammograms as a "second opinion" to assist a radiologist in detecting lesions and in making diagnosis decisions. Automated extraction of the breast region from mammograms is an important preprocessing step for the computer-aided diagnosis. By excluding the background region, further search operation for abnormalities are limited to the breast region. Without undue influence from the background region, the reliability and efficiency of further analysis can be improved. The segmentation algorithm should extract the breast region accurately and still be able to adapt itself to variations in digitizing systems, image orientations, image artifacts and other image characteristics.

There are two major problems associated with the accurate segmentation of the breast region. Due to the mammogram acquisition process, there is a region of decreasing contrast near the breast boundary, which leads to a lack of visibility along the breast contour in mammograms. Another problem is the non-uniform background region, which may also contain bright regions such as information labels or unexposed film regions.

Various approaches have been investigated to solve the problems effectively[3-9]. These approaches usually combine several techniques and set the parameters of the segmentation algorithm by trial and error. With the fixed parameter settings, they are subject to variation in performance with different kinds of mammograms and are necessitated of manual tuning of parameter

Received date: 2005-06-24; **Revised date**: 2005-07-02.

settings accordingly, which may be tedious and error-prone.

Due to the changes in image properties, the segmentation algorithm may need different sets of parameters for different images to obtain the optimal output. The usefulness of a set of parameters can only be determined by the output of the segmentation algorithm. To achieve robust performance, therefore, a need exists to apply learning techniques that can efficiently find parameter settings and yield optimal results for the given images.

In this paper we propose a learning-based approach for the automated segmentation. The approach uses an incremental method based on reinforcement learning for selecting parameter settings for the segmentation algorithm. The output of the segmentation algorithm is used as a feedback to influence the performance of the segmentation process. The approach adjusts the parameter settings of the segmentation algorithm according to the image properties through training and therefore adapts itself to various kinds of mammograms.

We develop a scheme to realize the automated segmentation. The scheme consists of two modules: the segmentation module and the learning module. The segmentation module extracts the breast region from the images. The percentage of area overlap between the output region and the template region in manual segmentation is computed as the reinforcement. The learning module uses the reinforcement to adaptively select the parameter settings that, when applied to the segmentation module, maximize the percentage overlap for the given image. The scheme is illustrated in Fig. 1.

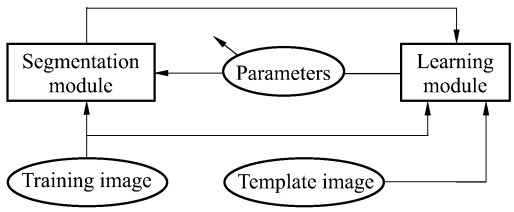

Fig. 1 Automated segmentation scheme based on reinforcement learning

The remainder of the paper is organized as follows: Section 2 presents the algorithm used in the segmentation module. Section 3 describes the reinforcement learning techniques and the learning algorithm adopted. Section 4 provides the experimental results for several kinds of mammograms. Section 5 concludes the paper.

2 Segmentation algorithm

The segmentation module uses the region-growing method to segment the breast region combined with the smooth filtering and the morphological filtering. Firstly, the image is preprocessed by the edge-preserving smooth filtering. Next, the smoothed homogeneous image is segmented using the region-growing segmentation algorithm. Finally, the segmented binary image is postprocessed by the binary morphological filtering, as illustrated in Fig. 2.

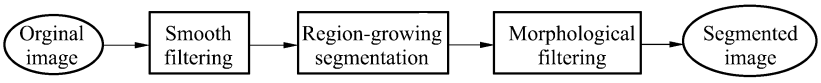

Fig. 2 Automated segmentation algorithm

2.1 Smooth filtering

The preprocessing smooth filtering can suppress the influence of noise. In order not to blur the edges in the image too much, we choose the bilateral filtering[10], which smoothes the image while preserving edges by means of a nonlinear combination of nearby image values. The method is non-iterative and local. It combines gray

levels based on both their geometric closeness and photometric similarity, and filters the image in both domain and range, which can be described as follows:

$$h(x) = k^{-1}(x)\int_{-\infty}^{\infty}\int_{-\infty}^{\infty} f(\xi)c(\xi,x)s(f(\xi),f(x))\mathrm{d}\xi$$

with the normalization

$$k(x) = \int_{-\infty}^{\infty}\int_{-\infty}^{\infty} c(\xi,x)s(f(\xi),f(x))\mathrm{d}\xi$$

where $f(x)$ and $h(x)$ denote the input image and the output image respectively. The closeness function $c(\xi,x)$ and the similarity function, $s(f(\xi),f(x))$ measure the geometric closeness and photometric similarity between the neighborhood center x and a nearby point ξ, respectively. We adopt the shift-invariant Gaussian filtering, in which both $c(\xi,x)$ and $s(f(\xi),f(x))$ are Gaussian functions of the Euclidian distance between their arguments. More specifically, c and s are radially symmetric

$$c(\xi,x)=\exp\left(-\frac{1}{2}\left(\frac{\mathrm{d}(\xi,x)}{\sigma_d}\right)^2\right)$$

where

$$\mathrm{d}(\xi,x)=\mathrm{d}(\xi,x)=\|\xi-x\|$$

and

$$s(f(\xi),f(x))=\exp\left(-\frac{1}{2}\left(\frac{\delta(f(\xi),f(x))}{\sigma_\delta}\right)^2\right)$$

where

$$\delta(f(\xi),f(x))=\delta(f(\xi)-f(x))=\|f(\xi)-f(x)\|$$

There are two parameters σ_d and σ_δ which are the geometric and photometric spread of the filter respectively to be set in the smooth filtering.

2.2 Region-growing segmentation

The homogeneous image smoothed by the bilateral filtering is then segmented using the region-growing method. On account of the global feature of the breast region, we use the connected threshold algorithm for the region-growing segmentation, which grows a region from seed pixels by labeling pixels that are connected to the seed pixels and lie within an intensity range. The lower and upper thresholds of the intensity range control the growing process, that is the neighboring pixel is labeled as a breast pixel if its intensity lies within the range or it is labeled as a background pixel otherwise. In our observations, the breast region always covers the center of a mammogram and has higher intensities. We therefore simply select the seeds to be the pixels with the highest gray level within a small region located at the center of a mammogram.

There are two parameters to be set in the connected threshold segmentation, the lower threshold, T_L, and upper threshold, T_U, of the intensity range.

2.3 Morphological filtering

The connected threshold algorithm outputs a segmented binary image. Because the border of the segmented region may be noisy, the resulting image is postprocessed by the binary morphological filtering. We use the standard morphological operations closing and opening[11] to smooth the border, which also remove small regions in the breast and background regions, respectively.

The closing and opening operations are performed by combining the elementary operations erosion and dilation according to the formulas

$$S_{\mathrm{closing}}I=S_{\mathrm{erosion}}(S_{\mathrm{dilation}}I),$$

and

$$S_{\text{opening}} I = S_{\text{dilation}}(S_{\text{erosion}} I).$$

where I is an image and S is a structuring element (a local neighborhood of any shape) applied to I. The erosion and dilation operations are defined by

$$S_{\text{erosion}} I = \min\{I(x-sx, y-sy) \mid \forall (sx, sy) \in S\}$$

and

$$S_{\text{dilation}} I = \min\{I(x+sx, y+sy) \mid \forall (sx, sy) \in S\}$$

We use the disk-shaped structuring elements for both closing and opening operations. The binary image is first processed by the closing operation and then by the opening operation. There are two parameters to be set in the morphological filtering. They are the diameter, D_C, of the closing structuring element, S_C, and the diameter, D_O, of the opening structuring element, S_O.

There are six parameters to be determined in the above segmentation algorithm. To reduce the search space of the learning algorithm, we roughly determine the sample ranges of the parameters in this work, which are listed in Tab. 1. The quantification level of images are supposed to be 256.

Tab. 1 Segmentation parameters and sample ranges

Parameters	Explanations	Sample ranges
σ_d	Geometric spread of bilateral filtering	1～9 (pixel)
σ_δ	Photometric spread of bilateral filtering	3～11 (grayscale)
T_L	Lower threshold of connected-threshold segmentation	1～32 (grayscale)
T_U	Upper threshold of connected-threshold segmentation	255 (grayscale)(fixed)
D_C	Diameter of structuring element of closing morphological filtering	3～9 (pixel)(odd number)
D_O	Diameter of structuring element of opening morphological filtering	11～21 (pixel)(odd number)

3 Learning algorithm

The learning module uses reinforcement learning techniques to learn the policy of selecting the parameter settings for the segmentation algorithm according to the image properties. The segmentation problem is posed as a Markov decision problem and is solved using the Q-learning algorithm.

3.1 Reinforcement learning

Reinforcement learning[12-13] studies computational approaches of learning from rewards and punishments (called reinforcements). It is about learning the optimal control policy in a Markov decision problem. A Markov decision problem is an abstract model of sequential decision problems, in which an agent interacts with the environment. In each decision cycle, the agent observes the environmental state and takes an action according to a policy. The action changes the environmental state and as a result the agent receives reinforcement from the environment. The value of this reinforcement depends on the environmental state, the decision, and possibly random disturbances. In this paper, the segmentation problem is cast as a Markov decision problem, in which the image properties represent the environmental states and the segmentation routines represent the actions.

There are two paradigms in reinforcement learning, associative and non-associative. In the

associative paradigm, the learning task has multiple stages of decisions and the reinforcement is often temporally delayed, occurring only after the execution of a sequence of decisions. In the non-associative paradigm, there is only one stage and the immediative reinforcement is received after each decision. In this paper, we use the non-associate paradigm, for it provides a simple, yet principled framework within which the main problems of the segmentation scheme of pipeline type can be properly addressed.

To characterize the image properties, we use the Fisher information measures in scale spaces as the environmental state. The Fisher information measure in scale spaces is the rate at which the entropy changes with image resolution. It is the weighted average of the spatial variation of image intensities and is invariant to rigid motions and is robust to noise. Details about the Fisher information measures in scale spaces can be found in[14-16].

The reinforcement corresponds to the percentage of area overlap between the extracted region of the algorithm and the template region of manual segmentation in mammograms. The percentage overlap is computed as the intersection divided by the union between the two regions,

$$(A \cap B)/(A \cup B),$$

where A and B are the sets of all pixels in the two regions respectively. Because the segmented images are binary, the set operations between two regions can be performed by logical operations between two binary images and summation over the resultant image.

3.2 *Q*-learning algorithm

The particular class of reinforcement learning methods employed in this work is the *Q*-learning algorithm[17-18]. *Q*-learning algorithm is an off-policy learning algorithm, in which the policy used for control and the policy to be evaluated and improved are separated so that the algorithm can evaluate one policy while following another policy. The policy used for control, called the behavior policy, may in fact be unrelated to the policy that is evaluated and improved, called the estimation policy. The advantage of this separation is that the estimation policy may be deterministic, while the behavior policy can continue to sample all possible actions.

The one-step *Q*-learning is defined by

$$Q(s_t, a_t) \leftarrow Q(s_t, a_t) + \alpha[r_{t+1} + \gamma \max_a Q(s_{t+1}, a) - Q(s_t, a_t)]$$

where Q is the action-value function, s is the state, a is the action, r is the resulting immediate reward, γ is the discounting factor, and α is the learning rate.

In this case, the learned action-value function, Q, directly approximates Q^*, the optimal action-value function, independent of the policy being followed.

Let i be an input image to the segmentation module, s_i be the properties of image i, and p be an instance of segmentation parameters. Then according to the *Q*-learning algorithm, $Q(s_i, p)$ measures how good the instance of p is when the segmentation algorithm is applied to image i. When the *Q*-learning algorithm is applied to the parameters, the value of $Q(s_i, p)$ will be evaluated and improved to approximate the optimal value.

Fig. 3 gives the main steps of the algorithm described above, where the softmax policy is an exploratory policy that selects actions according to a distribution. The inner loop of the algorithm terminates when either the number of iterations has exceeded a prescribed value or the average percentage overlap has reached a given threshold.

* Initialization: $Q(s_x, p) \leftarrow 0$ for all x and p, where x is an image and p is an instance of segmentation parameters.
* LOOP:
  (1) For each image i in the training set, DO
  (a) Computed the image properties s_i.
  (2) LOOP:
  (a) Segment image i with parameters p recommended by the softmax policy.
  (b) Compute the percent overlap between the output region and the template region of manual segmentation as the reinforcement r.
  (c) Update: $Q(s_i, p) \leftarrow Q(s_i, p) + \alpha[r - Q(s_i, p)]$
  (3) UNTIL terminating condition.
* UNTIL all images has been trained.

Fig. 3 Main steps of the learning algorithm for adjustment of segmentation parameters

4 Experimental results

There are several representation schemes for the Q function in reinforcement learning. To speed up the convergence of learning process, we use a lookup-table representation. The two dimensions of the lookup table are the image properties and a particular combination of parameter settings. Also, scale level of images $L=4$, maximum number of iterations $N=100$, threshold of average percent overlap $R=99\%$, Gibbs distribution used for the softmax policy, and $\alpha=0.1$ for all experiments reported here.

The algorithm is trained and tested on all 322 mammograms from the MIAS database[19]. Each of the mammograms is manually segmented into the breast and background regions for quantitative training and testing. The mammograms have been reduced in resolution to 400 μm to facilitate fast and efficient processing. To demonstrate the adaptability of the approach, it has been trained and tested on mammograms with different background tissues: fatty, fatty glandular and dense glandular respectively. For each kind of background tissue, the images are randomly divided into two groups, one for training and the other for testing.

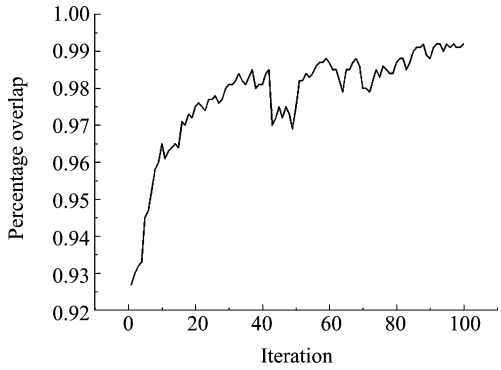

Fig. 4 Training results for MIAS image mdb005

Fig. 4 shows how the percentage of overlap changes with iterations in the training process on an image. It should be noted that over iteration the percentage of overlap increases incrementally.

To illustrate the results further, three cases of test results on mammograms with different background tissues are shown in Fig. 5～7. The images show the original mammogram, the extracted breast region represented by a binary image, and the contour superimposed on a LOG-attenuated version of the original image. In addition, the learned segmentation parameters are also listed.

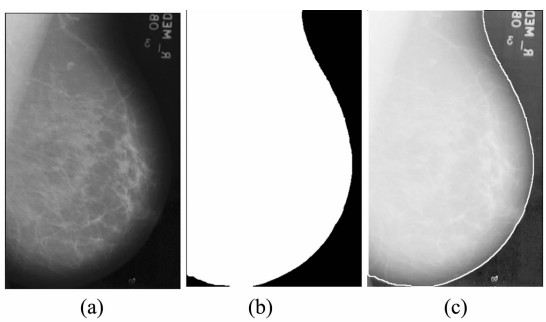

Fig. 5 Test results for MIAS image mdb232 (fatty tissue): (a) Original image, (b) Extracted region, (c) Contour overlain on a LOG-attenuated version of (a). The learned segmentation parameters are: $\sigma_d=1$, $\sigma_\delta=3$, $T_L=9$, $T_U=255$, $D_C=3$, $D_O=11$.

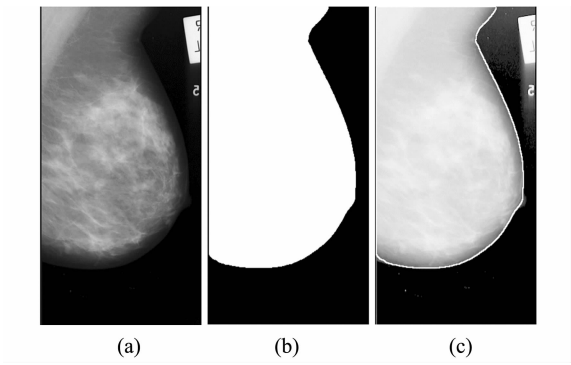

Fig. 6 Test results for MIAS image mdb016 (fatty glandular tissue): (a) Original image, (b) Extracted region, (c) Contour overlain on a LOG-attenuated version of (a). The learned segmentation parameters are: $\sigma_d = 2, \sigma_\delta = 5, T_L = 21, T_U = 255, D_C = 5, D_O = 17$.

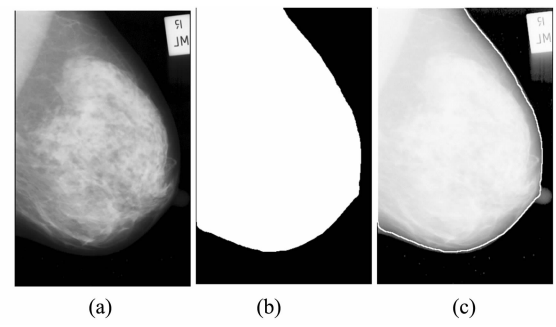

Fig. 7 Test results for MIAS image mdb126 (dense glandular tissue): (a) Original image, (b) Extracted region, (c) Contour overlain on a LOG-attenuated version of (a). The learned segmentation parameters are: $\sigma_d = 3, \sigma_\delta = 4, T_L = 24, T_U = 255, D_C = 3, D_O = 21$.

Besides the visual evaluation of test results to assure that the extracted region approximately matches the breast region, quantitative test results are also computed and listed in Tab. 2.

Tab. 2 Test results on MIAS mammogram database

Background tissue	Number of images	Mean of percent overlap	Standard deviation of percent overlap	Minimum of percent overlap
Fatty	106 total 53 for testing	97.3%	2.3%	94.4%
Fatty glandular	104 total 52 for testing	97.4%	2.2%	94.7%
Dense glandular	112 total 56 for testing	96.6%	2.8%	92.3%

For three groups of mammograms of different background tissues, the mean of percentage of overlap is 97.1% and the average standard deviation is 2.4%. The test results indicate that the extracted region approximately matches the manually segmented region. Through analysis of the poorly segmented images, we find that the main reason for the poor segmentation is the artifacts caused by the digitizing process. Removing these artifacts by a preprocessing step can further improve the segmentation results. The relatively large variance may be caused by the discretization of image properties, which influences the generalization of the learning algorithm. One possible solution is to use the function approximator such as kernel functions[20] to represent the Q function. The computational burden and training time will increase accordingly.

Comparison of the test results to previously published results is difficult because of the variations in mammogram databases the number, of images and the evaluation method. Most of the previous results are subjective and based on visual evaluation. Those with quantitative results differ in image database and evaluation method. The approach in[9], which has an evaluation method is similar to ours, is tested on 25 mammograms from the MIAS database and the average error is 2.7%. However, our approach is more adaptive to the automated segmentation and does not require the tuning of parameter settings manually. Through training, the performance of the approach can be improved incrementally.

5 Conclusions

The automated segmentation approach based on reinforcement learning described in this paper shows its adaptability to several kinds of digital mammograms in experiments. The proposed approach uses segmentation results as feedbacks to influence the performance of the segmentation algorithm in a systematic way, which selects the parameter settings according to the image properties so as to adapt itself to various kinds of mammograms. One additional benefit of the approach, due to the stochastic nature of reinforcement learning, is that it can explore a significant portion of the parameter space, resulting in the discovery of good solutions, which makes it unnecessary of manual tuning of parameter settings. To improve the performance further, preprocessing step of removing digitizing artifacts and refining representation of Q function will be considered in future work.

References:

[1] KARSSEMEIJER N, HENDRIKS J H. Computer-assisted reading of mammograms[J]. *Europe Radiology*, 7: 743-748, 1997.

[2] JIANG Y, NISHIKAWA R M, SCHMIDT R A, METZ C E, GIGER M L, DOI K. Improving breast cancer diagnosis with computer-aided diagnosis[J]. *Academic Radiology*, 1999,6:22-33.

[3] BICK U, GIGER M L, SCHMIDT R A, NISHIKAWA R M, WOLVERTON D E, DOI K. Automated segmentation of digitized mammograms[J]. *Academic Radiology*, 1995,2:1-9.

[4] CHANDRASEKHAR R, ATTIKIOUZEL Y. Gross segmentation of mammograms using a polynomial model[C]. *International Conference of the IEEE Engineering in Medicine and Biology Society. Amsterdam, Netherlands*, 1996,3:1056-1058.

[5] HEINE J J, KALLERGI M, CHETELAT S M, CLARKE LP. Multiresolution wavelet approach for separating the breast region from the background in high resolution digital mammography[C]. *Digital Mammography* 98, *Karssemeijer N (eds.), Dordrecht, Kluwer*, 1998:295-298.

[6] CHANDRASEKHAR R, ATTIKIOUZEL Y. Automatic breast border segmentation by background modeling and subtraction[C]. *The* 5th *International Workshop on Digital Mammography, Yaffe MJ (eds.). Medical Physics Publishing, Toronto, Canada*, 2000,560-565.

[7] LOU S L, LIN H D, LIN K P, HOOGSTRATE D. Automatic breast region extraction from digital mammograms for PACS and telemammography applications[J]. *Computerized Medical Imaging and Graphics*, 2000, 24: 205-220.

[8] OJALA T, NAPPI J, NEVALAINEN O. Accurate segmentation of the breast region from digitized mammograms [J]. *Computerized Medical Imaging and Graphics*, 2001,25:47-59.

[9] WIRTH M A, STAPINSKI A. Segmentation of the breast region in mammograms using active contours[C]. *Visual Communications and Image Processing, Ebrahimi T, Sikora T (eds.), Lugano, Switzerland*, 2003, 5150: 1995-2006.

[10] TOMASI C, MANDUCHI R. Bilateral filtering for gray and color Images[C]. *Proceedings of the* 1998 *IEEE International Conference on Computer Vision, Bombay, India*, 1998.

[11] GONZALEZ R C, WOODS R E. *Digital image processing*[M]. 2nd edition. Prentice Hall, 1992.

[12] KAELBLING L P, LITTMAN M L, MOORE A W. Reinforcement learning: a survey[J]. *Journal of Machine Learning Research*, 1996, 4: 237-285.

[13] SUTTON R S, BARTO A G. *Reinforcement learning: an introduction*[M]. MIT Press, 1998.

[14] HADJIDEMETRIOU E, GROSSBERG M D, NAYAR S K. Multiresolution histogram and their use for recognition[J]. *IEEE Transactions on Pattern Analysis and Machine Intelligence*, 2004, 26: 831-874.

[15] HADJIDEMETRIOU E, GROSSBERG M D, NAYAR S K. Spatial information in multiresolution histograms

[C]. *Proceedings of IEEE Conference on Computer Vision and Pattern Recognition*, *Hawaii*, 2001,1:702-709.

[16] SPORRING J, WEICKERT J. Information measures in scale-spaces[J]. *IEEE Transactions on Information Theory*, 1999,45:1051-1058.

[17] WATKINS C. *Learning from delayed rewards*[D]. PhD thesis, Cambridge University, Cambridge, England, 1989.

[18] WATKINS C, DAYAN P. Q-learning[J]. *Machine Learning*, 1992,8:279-292.

[19] SUCKLING J, PARKER J, DANCE D R, *et al*. *The Mammographic Image Analysis Society digital mammogram database*[R]. The 2nd International Workshop on Digital Mammography, Gale AG, Astley SM, Dance DR, Cairns AY (eds.), Elsevier, York, England, 1994,375-378.

[20] ORMONEIT D, SEN S. Kernel-based reinforcement learning[J]. *Machine Learning*,2002,49:161-178.

Brief professional biography of the author:

LIU Xin-yue is currently a PhD student at Changchun Institute of Optics, Fine Mechanics and Physics, Chinese Academy of Sciences. His research is focused on medical image analysis and machine learning.